Supplementary Information (SI) for New Journal of Chemistry.

Supporting Information

Spectroscopic Behaviours of a Newly Synthesized Benzimidazole Probe (EBINP) with Native and Denatured Bovine Serum Albumin Supported by Docking and Molecular Dynamics

Shreya Roy,[a] Dr. Titas K. Mukhopadhyay,[a] Madan Sau,[b] Sapana Dubey,[a] Gulfisha,[a] Keshav Basudev,[a] Subhabrata Nayak,[c] Gokarneswar Sahoo,[c] Dr. Subrata Mahanta,*[a] Dr. Tapas Das,*[a]

---

a Department of Chemistry
National Institute of Technology Jamshedpur
Jamshedpur-831014, India
tapas.chem@nitjsr.ac.in
b Environment Analyst
West Bengal Pollution Control Board
Darjeeling-734010
c Department of Chemistry
National Institute of Technology Rourkela
Rourkela-769008, India

1. Materials and General Methods:

All reactions were carried out in oven dried glassware with magnetic stirring. All solvents were purified and dried according to standard methods prior to use. Starting materials alkyl-3-(2-formylnapthalen-1-yl)propanoate were prepared by reported methods.[1] ^1H spectra were recorded on BRUKER 400 MHz in $CDCl_3$ and ^{13}C NMR spectra were recorded on 100 MHz in $CDCl_3$ using TMS or residual solvent signals as internal standard. Data for ^1H NMR are recorded as follows: chemical shift (δ, ppm), multiplicity (s = singlet, d = doublet, t = triplet, q = quartet, m = multiplet or unresolved, coupling constant(s) in Hz, integration). Data for ^{13}C NMR are reported in terms of chemical shift (δ, ppm). High resolution mass spectra (HRMS) were obtained by the ESI (Q-TOF) ionization sources. Routine monitoring of reactions was performed using precoated silica gel TLC plates from E-Merck. All the chromatographic separations were carried out by using silica gel (Acme's, 100-200 mesh). For the measurement of absorption, a LABINDIA UV 3200 XE UV/vis spectrophotometer was used, and for the emission study, PerkinElmer fluorescence spectrophotometer FL 6500 instruments were used to study the samples. In the fluorometer, an excitation slit width of 2.5 nm and an emission slit width of 10 nm were used. The excited state fluorescent lifetime measurement was carried out on Horiba Jobin Yvon Deltaflex, Springer New York, 2006, using a picosecond laser diode of 314 nm.

Quantum yield (Q) of a fluorophore is calculated by the conventional optical method, based on eq. S1.[2]

$$Q_2 = Q_1 \times \frac{\int F_2(\lambda)d\lambda}{\int F_1(\lambda)d\lambda} \times \frac{A_1(\lambda)}{A_2(\lambda)} \times \frac{{n_2}^2}{n_1^2} \qquad \text{eq. S1}$$

Suffixes 1 and 2 refer to standard and EBINP, respectively. Here quantum yields, integrated fluorescent intensities, absorbances, and refractive indexes of the medium are denoted by Q, $\int F(\lambda)d\lambda, .A(\lambda)\ and\ n$, respectively.

As per the requirement, the emission data were fitted at double, triple, or quadruple exponential function monitoring 400 nm wavelength best on eq. S2.[3]

$$F(t) = a_0 + a_1e^{(-t/\tau_1)} + a_2e^{(-t/\tau_2)} + a_3e^{(-t/\tau_3)} + a_4e^{(-t/\tau_4)} \qquad \text{eq. S2}$$

The time shift between sample decay and IRF (Instrument Response Function) is denoted by τ_1, τ_2, τ_3, and τ_4 are different lifetime components of different characteristic excited states with amplitudes a_1, a_2, a_3, and a_4, respectively. The average fluorescence lifetime is given by eq. S3.

$$\tau_{av} = <\tau> = \sum_i a_i \tau_i / \sum_i a_i \qquad \text{eq. S3}$$

2. General procedure for the synthesis of Alkyl-3-(2-(1H-benzo[d]imidazol-2-yl)naphthalen-1-yl)propanoate:

We prepared compound **4** following our previous literature procedure.[1]

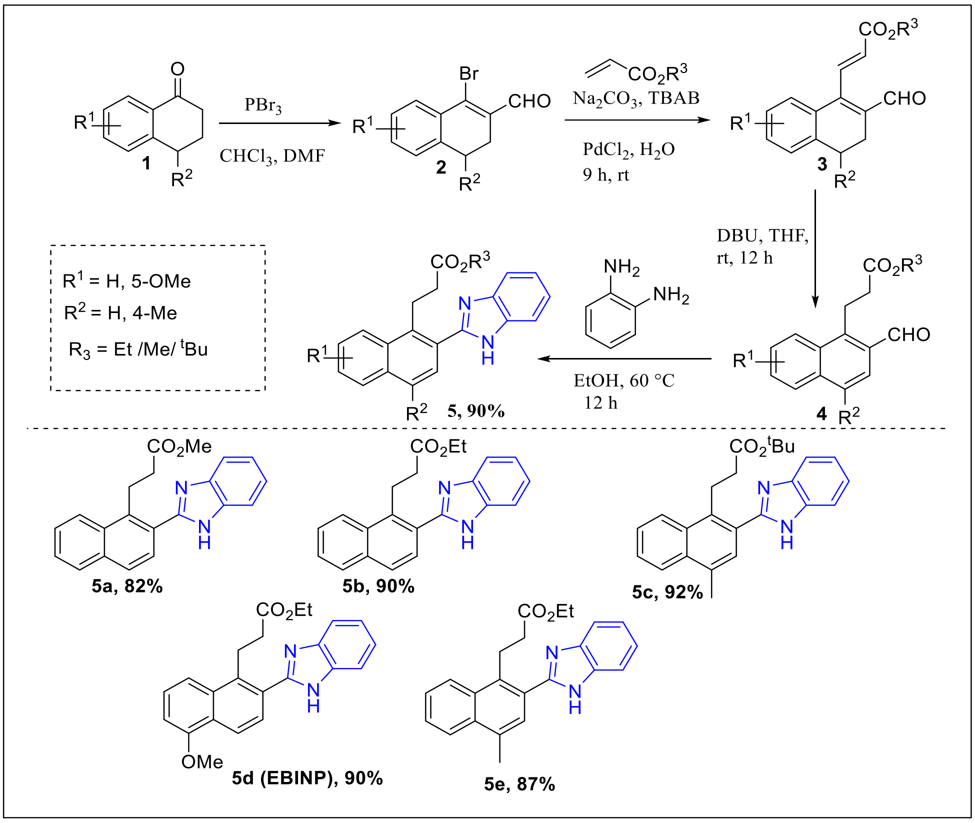

Scheme S1. Preparation of benzimidazole compounds from α-tetralone.

Methyl 3-(2-(1H-benzo[d]imidazol-2-yl)naphthalen-1-yl)propanoate (5a) (25 mg , 0.134 mmol, 1.0 equiv.) was taken in a pressure tube, 1.5 ml EtOH was added as a solvent and benzene-1,2-diamine (14 mg, 0.134 mmol, 1.0 equiv.) was added, the reaction mixture was stirred for 12 hours at 60 °C temperature. After 12 hours the resulting reaction mixture was dried under reduced pressure. the reaction mixture was diluted with 20 ml of EtOAc and the organic phase was separated from the aqueous phase. The aqueous phase was extracted from EtOAc (2 x 15 ml), the combined organic phase was dried over anhydrous Na_2SO_4, filtered and concentrated under reduced pressure. The crude residue was purified by silica gel column chromatography (10% of EtOAc in hexane) to obtain a yellow amorphous solid product (37 mg, 0.112 mmol, 82 % yield). **^{1}H NMR (400 MHz, $CDCl_3$)** δ 8.03 (d, *J* = 7.8 Hz, 1H), 7.92 – 7.84 (m, 1H), 7.70 (d, *J* = 9.0 Hz, 4H), 7.64 – 7.52 (m, 2H), 7.34 – 7.26 (m, 2H), 3.64

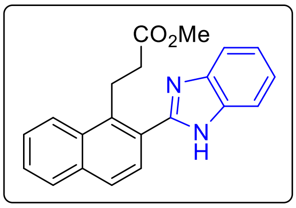

(s, 3H), 3.59 (t, *J* = 7.2 Hz, 2H), 2.97 (t, *J* = 7.1 Hz, 2H). **^{13}C NMR (101 MHz, CDCl$_3$)** δ 174.7, 152.5, 135.6, 134.2, 132.1, 131.6, 130.6, 129.0, 128.2, 127.5, 127.4, 126.8, 126.6, 124.4, 122.6, 52.0, 34.8, 24.3. **HRMS cald**. for $C_{21}H_{18}N_2O_2$: $(M+H)^+$ 330.1368; found: 330.1747

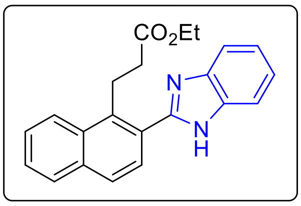

Ethyl 3-(2-(1H-benzo[d]imidazol-2-yl)naphthalen-1-yl)propanoate (5b) was obtained as a yellowish amorphous solid in 90 % yield. **^{1}H NMR (500 MHz, CDCl$_3$)** δ 8.02 (d, *J* = 8.3 Hz, 1H), 7.86 (d, *J* = 8.2 Hz, 1H), 7.72 (s, 2H), 7.69 (s, 2H), 7.56 (ddd, *J* = 15.5, 14.0, 6.8 Hz, 2H), 7.31 – 7.26 (m, 2H), 4.07 (q, *J* = 7.1 Hz, 2H), 3.58 (t, *J* = 7.3 Hz, 2H), 2.96 (t, *J* = 7.3 Hz, 2H), 1.13 (t, *J* = 7.1 Hz, 3H). **^{13}C NMR (126 MHz, CDCl$_3$)** δ 174.5, 152.5, 135.5, 134.2, 131.6, 129.0, 128.2, 127.6, 127.4, 126.8, 126.6, 124.5, 122.6, 61.0, 35.1, 24.3, 14.0. **HRMS cald**. For $C_{22}H_{20}N_2O_2$: $(M+H)^+$ 344.1525; found: 344.1530

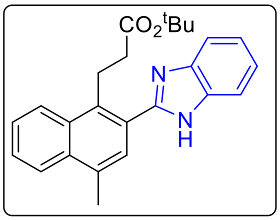

Tert-butyl 3-(2-(1H-benzo[d]imidazol-2-yl)-4-methylnaphthalen-1-yl)propanoate (5c) was obtained as an off-white amorphous solid in 92 % yield. **^{1}H NMR (400 MHz, CDCl$_3$)** δ 11.93 (s, 1H), 8.08 (dd, *J* = 6.4, 3.2 Hz, 2H), 7.73 (s, 2H), 7.62 (dd, *J* = 6.4, 3.3 Hz, 3H), 7.35 – 7.29 (m, 2H), 3.57 (t, *J* = 7.1 Hz, 2H), 2.96 (t, *J* = 7.1 Hz, 2H), 2.67 (s, 3H), 1.32 (s, 9H). **^{13}C NMR (101 MHz, CDCl$_3$)** δ 174.6, 152.8, 133.7, 133.6, 133.2, 131.9, 128.6, 128.0, 126.3, 126.3, 125.2, 125.1, 81.7, 36.3, 27.9, 24.2, 19.3. **HRMS cald**. For $C_{25}H_{26}N_2O_2$: $(M+H)^+$ 386.1994; found: 386.2074

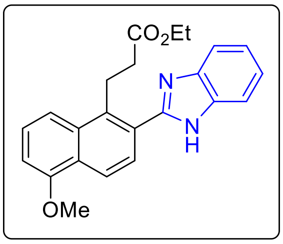

Ethyl 3-(2-(1H-benzo[d]imidazol-2-yl)-5-methoxynaphthalen-1-yl)propanoate (5d) was obtained as a white amorphous solid in 90 % yield. **^{1}H NMR (400 MHz, CDCl$_3$)** δ 11.29 (s, 1H), 8.29 (d, *J* = 8.8 Hz, 1H), 7.87 (s, 1H), 7.79 (d, *J* = 8.8 Hz, 1H), 7.65 (d, *J* = 8.7 Hz, 1H), 7.59 (s, 1H), 7.52 (t, *J* = 8.2 Hz, 1H), 7.36 – 7.29 (m, 2H), 6.92 (d, *J* = 7.6 Hz, 1H), 4.11 (q, *J* = 7.1 Hz, 2H), 4.05 (s, 3H), 3.64 (t, *J* = 7.3 Hz, 2H), 3.02 (t, *J* = 7.3 Hz, 2H), 1.18 (t, *J* = 7.1 Hz, 3H). **^{13}C NMR (101 MHz, CDCl$_3$)** δ 174.6, 156.1, 152.6, 135.0, 132.8, 128.8, 126.9, 126.8, 126.4, 121.4, 116.7, 104.6, 61.0, 55.66, 35.1, 24.7, 14.1. **HRMS cald**. For $C_{23}H_{22}N_2O_3$: $(M+H)^+$ 374.1630; found: 374.1730

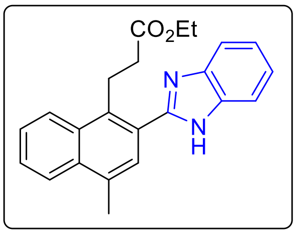

Ethyl 3-(2-(1H-benzo[d]imidazol-2-yl)-4-methylnaphthalen-1-yl)propanoate (5e) was obtained as an off-white amorphous solid in 87 % yield. **^{1}H NMR (400 MHz, CDCl$_3$)** δ 11.53 (s, 1H), 8.09 (dt, *J* = 5.5, 3.4 Hz, 2H), 7.87 (s, 1H), 7.71 (s, 1H), 7.66 – 7.58 (m, 3H), 7.35 – 7.29 (m, 2H), 4.11 (q, *J* = 7.1 Hz, 2H), 3.63 (t, *J* = 7.1 Hz, 2H), 3.03 (t, *J*

= 7.1 Hz, 2H), 2.69 (s, 3H), 1.17 (t, *J* = 7.1 Hz, 3H). **^{13}C NMR (101 MHz, CDCl$_3$)** δ 174.8, 152.7, 133.8, 133.6, 133.3, 131.8, 128.4, 128.0, 126.4, 125.1, 125.0, 61.1, 35.2, 24.1, 19.3, 14.0. **HRMS cald**. For $C_{23}H_{22}N_2O_2$: $(M+H)^+$ 358.1681; found: 358.1760

3. Behaviour of EBINP in mixed solvent (Water-Acetonitrile) system:

Water and acetonitrile volume ratios are varied from 0 to 100%. It was observed that on increasing the percentage of water in the binary mixture i.e, with increasing the dielectric constant of the medium[4] (Table-S1), the absorbance as well as emission intensity gradually decreased. Notably, red shifting of the emission spectra was observed by about 75 nm (Figure S2) on increasing percentage of water in acetonitrile (individually in acetonitrile and in water medium emission maxima at 400 nm and 475 nm respectively); but in the absorption spectra slight blue shift noticed (Figure S1). The decrease in absorption and emission intensity might be due to the aggregation and nonplanarity of the substrate.

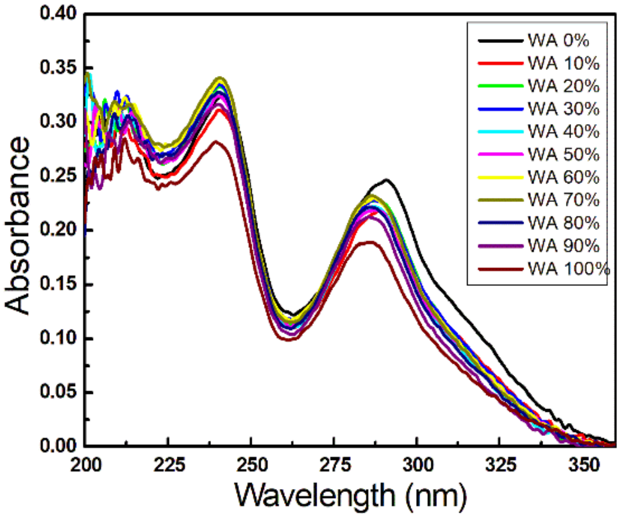

Figure S1. Absorption spectra of EBINP in mixed solvent systems (Concentration of EBINP is 8.49 μM)

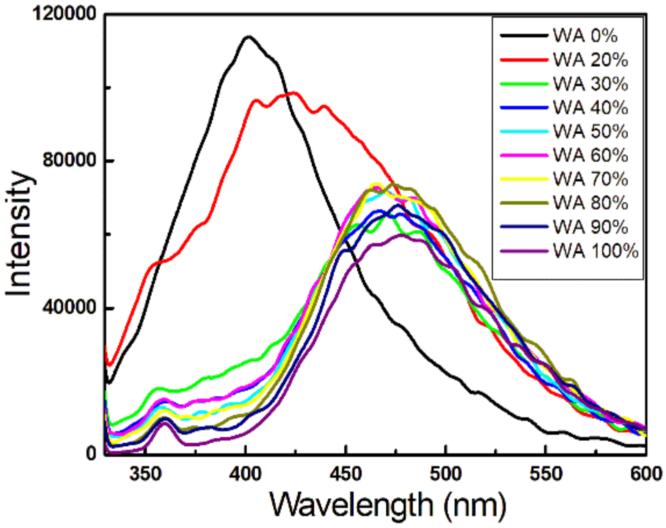

Figure S2. Emission spectra of EBINP in mixed solvent systems (Concentration of EBINP is 0.128 μM)

Table S1. variation of λ_{max} with dielectric constant

Water % (v/v)	Acetonitrile % (w/w)	Experimental dielectric constant	λ_{max} (absorption) (nm)	λ_{max} (emission) (nm)
0	100	76.5	320	400
10	70.48	76.19	318	421
20	31.36	75.89	317	464
30	18.27	75.5	317	471
40	11.75	74.79	317	472
50	7.83	74.1	317	472
60	5.22	72.6	317	473
70	3.36	69.69	317	474
80	1.95	63.48	316	475
90	0.87	45.78	314	475
100	0	35.15	313	475

4. Study of the behaviour of EBINP in acidic and in basic medium:

We investigated the behaviour of EBINP in acidic and basic medium. In this study the concentration of EBINP was maintained at 8.49 μM for absorption spectra and 0.128 μM for emission spectra. Figure S3 demonstrates that the absorbance and emission are unaffected by the addition of 0.25M AcOH to the water medium. The emission λ_{max} was set at 475 nm (Figure S3(b)) and the absorption λ_{max} at 320 nm (Figure S3(a)). Upon addition of 0.25 M NaOH in aqueous medium, the absorption spectra (Figure S4(a)) remained unchanged, but the emission intensity decreased and the emission λ_{max} moved from 475 nm to 410 nm via an isoemissive point (Figure S4(b)). A new, tiny absorption band at 340 nm is observed when 0.25 M AcOH is added to acetonitrile medium (Figure S5(a)) and the 390 nm band in the emission spectra shifts to 475 nm (Figure S5(b)), with the increment in intensity. The emission maxima shifted from 386 nm to 440 nm (Figure S6(b)) and the absorption λmax was somewhat pushed towards the longer wavelength area (Figure S6(a)) when 1M aqueous NaOH was added to an acetonitrile solution.

We may infer from the study of these spectra that our probe EBINP is protonated when acid or water is present; in this scenario, water may serve as a proton source for the probe (Scheme S2), which explains why the emission maxima in the water medium and the AcOH media are identical. Our probe is composed of two parts: the naphthyl ring component and the benzimidazole part. The benzimidazole part functions as LUMO and the naphthyl ring part as HOMO. Therefore, the positive charge generated in the imidazole ring facilitates HOMO to LUMO electron transfer, when the imidazole nitrogen is protonated. Because of this, redshift occurs upon water or acid addition with enhancement of the fluorescence intensity. The situation is intriguingly altered in the basic condition. The imidazole ring's positive charge is initially neutralized in a water medium when base is added; at that time, the isoemissive point at 437 nm is obtained. When the addition of acid was initiated in the acetonitrile medium, this isoemissive point was present; the probe was proceeding to the protonated state through this point. Following the withdrawal of the N-H-bonded proton by OH^{-}, a negative charge is generated on the benzimidazole ring (Scheme S2), which reduces HOMO to LUMO electron transfer efficiency and causes a blue shift. Prior to employing the base, the probe was in its non-ionized state in an acetonitrile medium. The onset of base addition results in the withdrawal of an N-H proton and the development of a negative charge on N. Meanwhile, acetonitrile and aqueous NaOH undergo a reaction, ultimately forming carboxylic acid.[5] As a result negative charge in the solution will be less noticeable due to the acid's production (Scheme S2); the HOMO-LUMO electron transition has been facilitated once more, increasing the intensity of spectra, and shifting the λ_{max} towards the red region.

Addition of acid in water medium

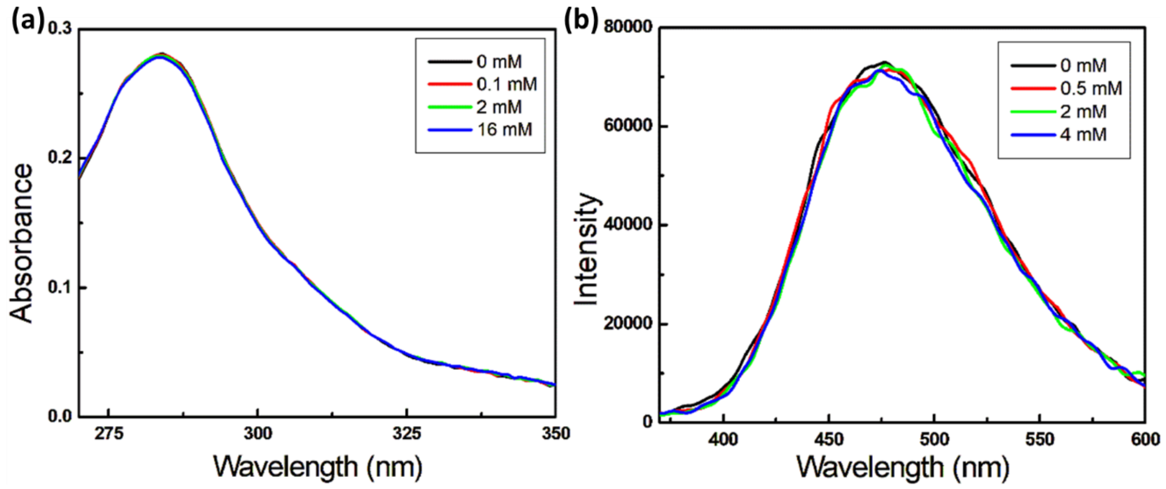

Figure S3. (a) absorption spectra and (b) emission spectra (λ_{exc} 320 nm) of EBINP in gradual addition of AcOH (0.25 M) in water medium.

Addition of base in water medium

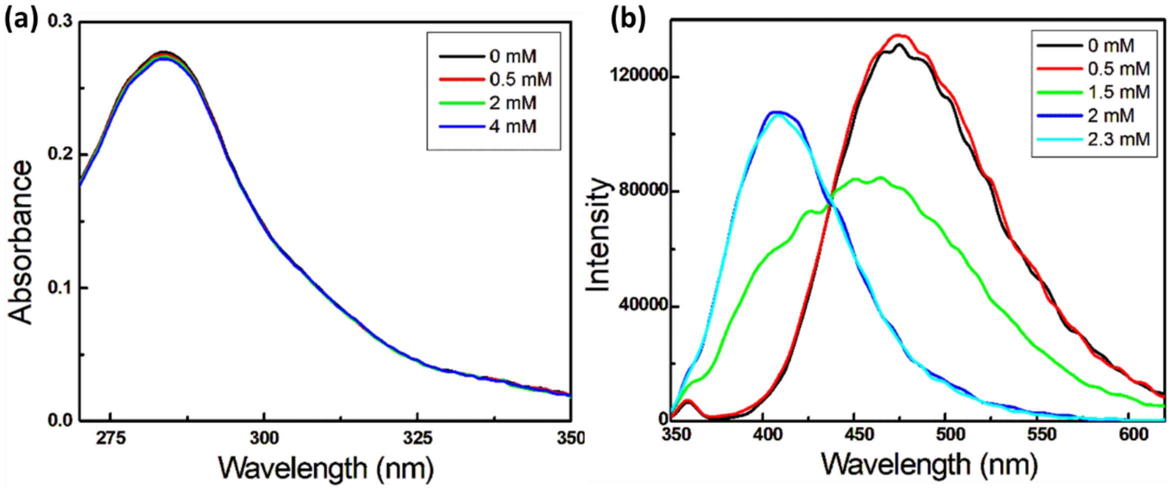

Figure S4. (a) absorption spectra and (b) emission spectra (λ_{exc} 320 nm) of EBINP in gradual addition of NaOH (0.25 M) in water medium.

Addition of acid in acetonitrile medium

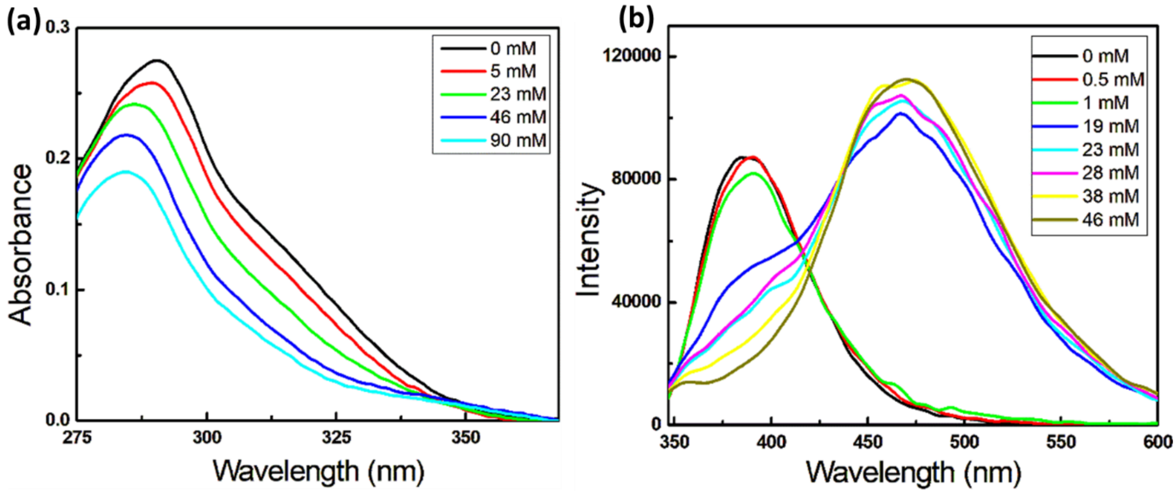

Figure S5. (a) absorption spectra and (b) emission spectra (λ_{exc} 320 nm) of EBINP in gradual addition of AcOH (0.25 M) in ACN medium.

Addition of base in acetonitrile medium

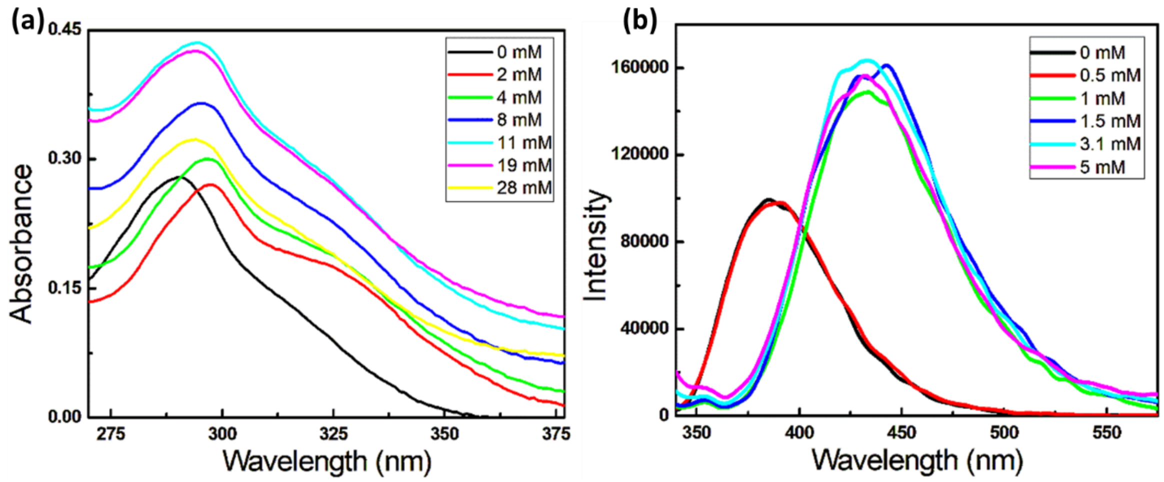

Figure S6. (a) absorption spectra and emission spectra (λ_{exc} 320 nm) of EBINP in gradual addition of NaOH (0.25 M) in ACN medium.

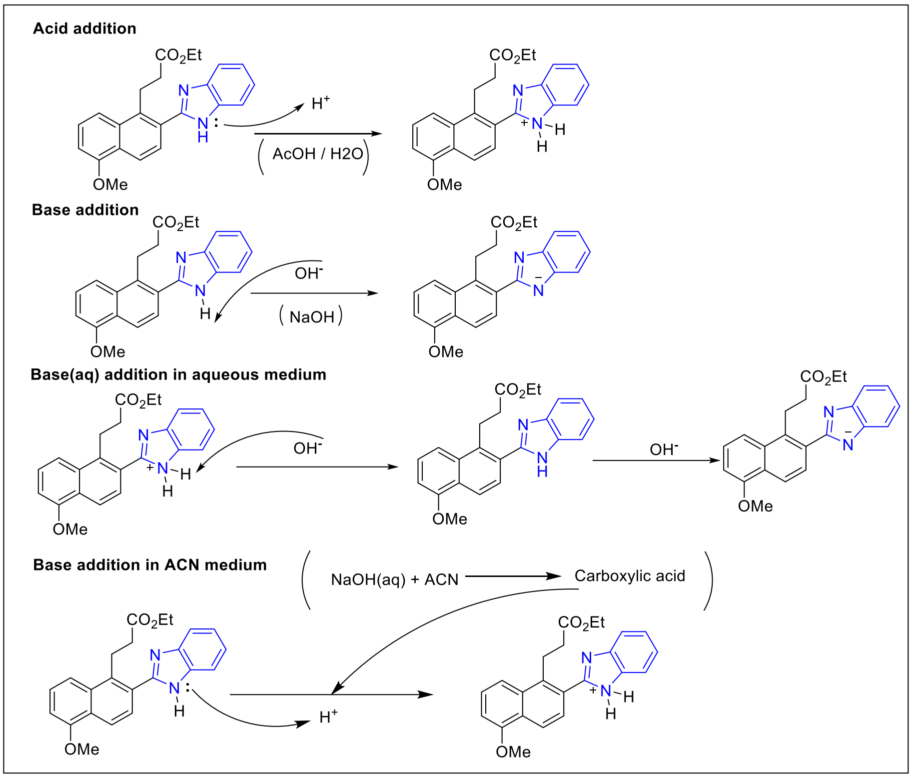

Scheme S2. Acid base effect on benzimidazole moiety.

5. ^{1}H and ^{13}C NMR of benzimidazole compounds:

^{1}H and ^{13}C NMR of compound 5a

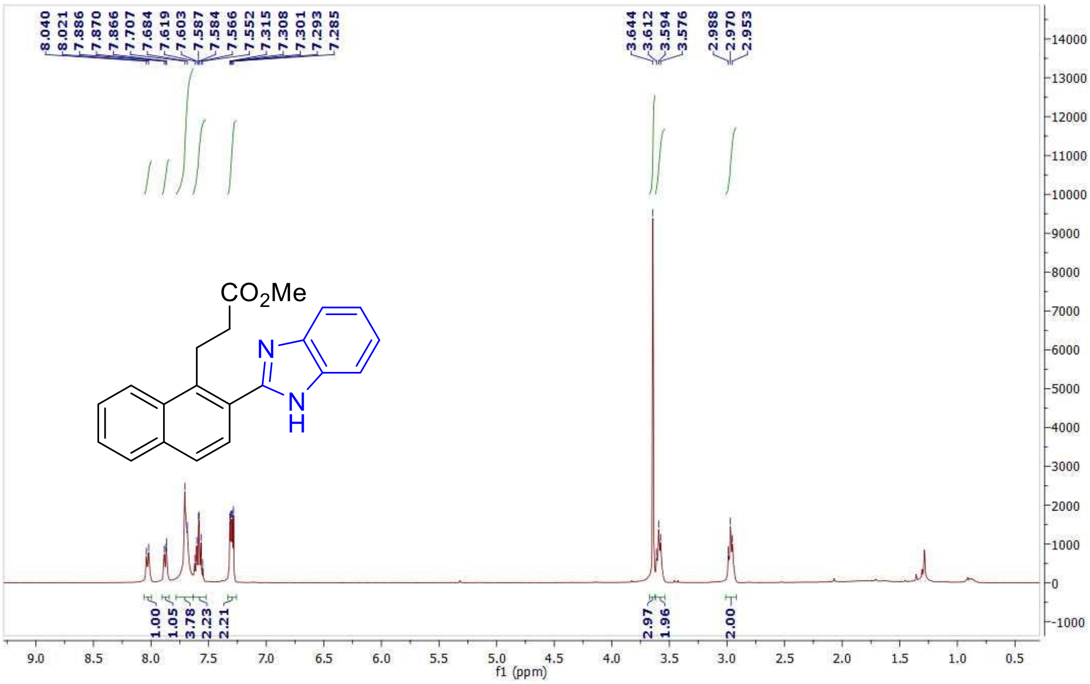

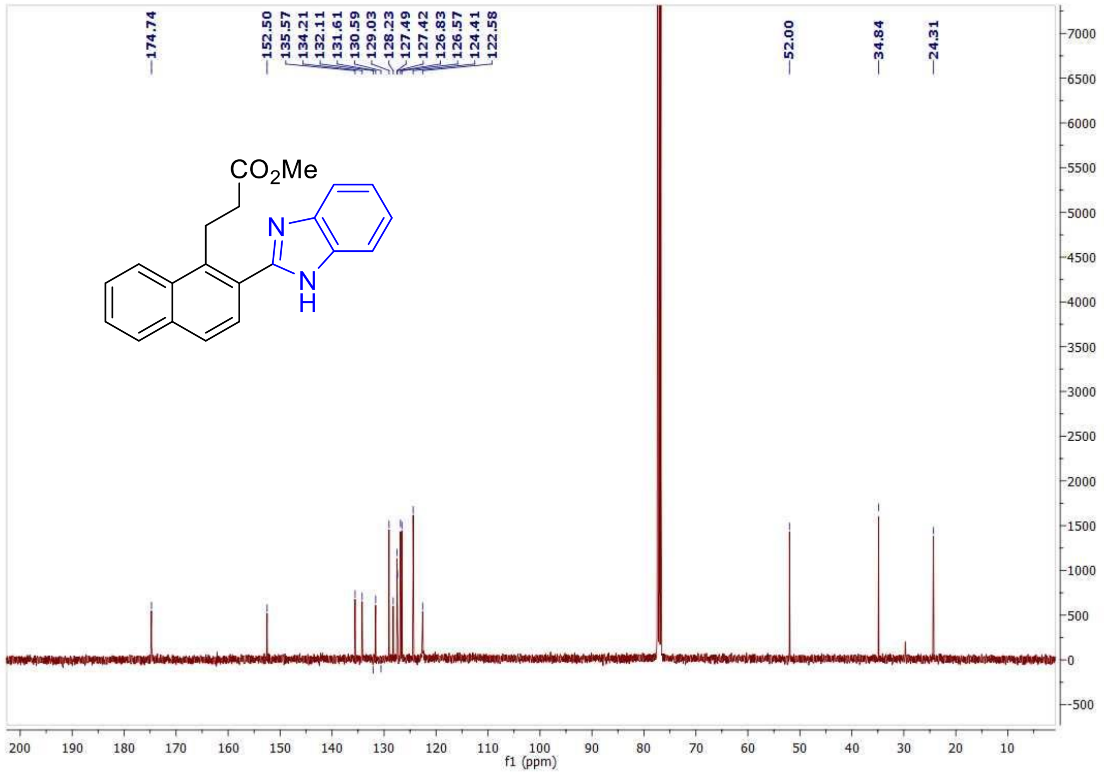

^{1}H and ^{13}C NMR of compound 5b

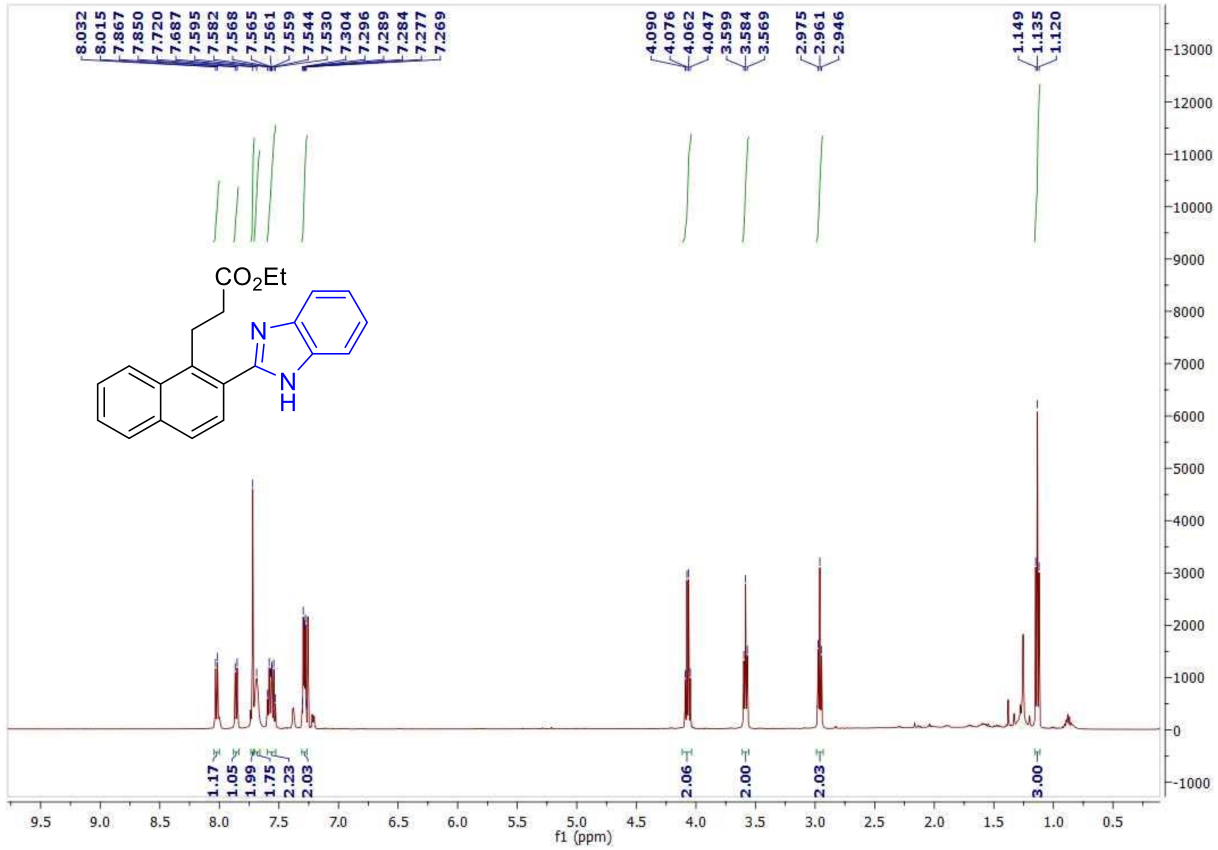

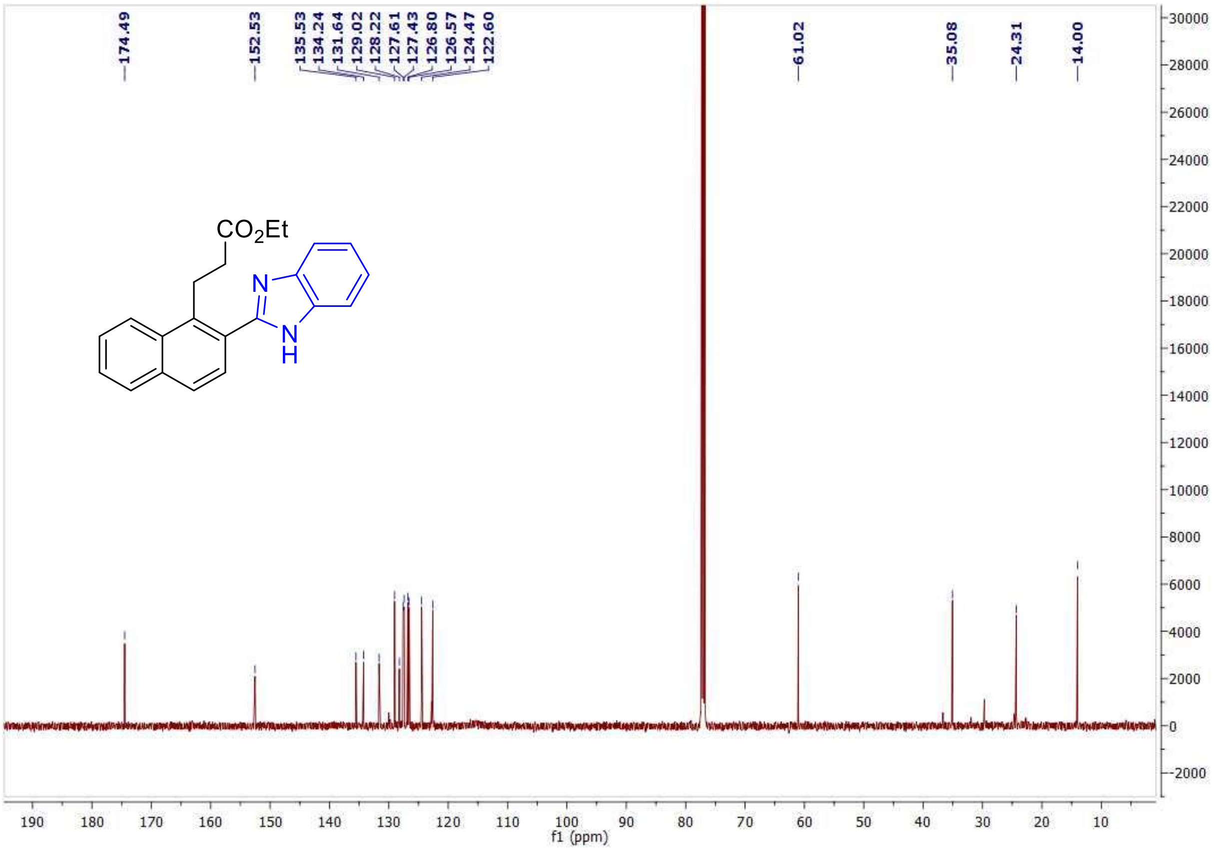

^{1}H and ^{13}C NMR of compound 5c

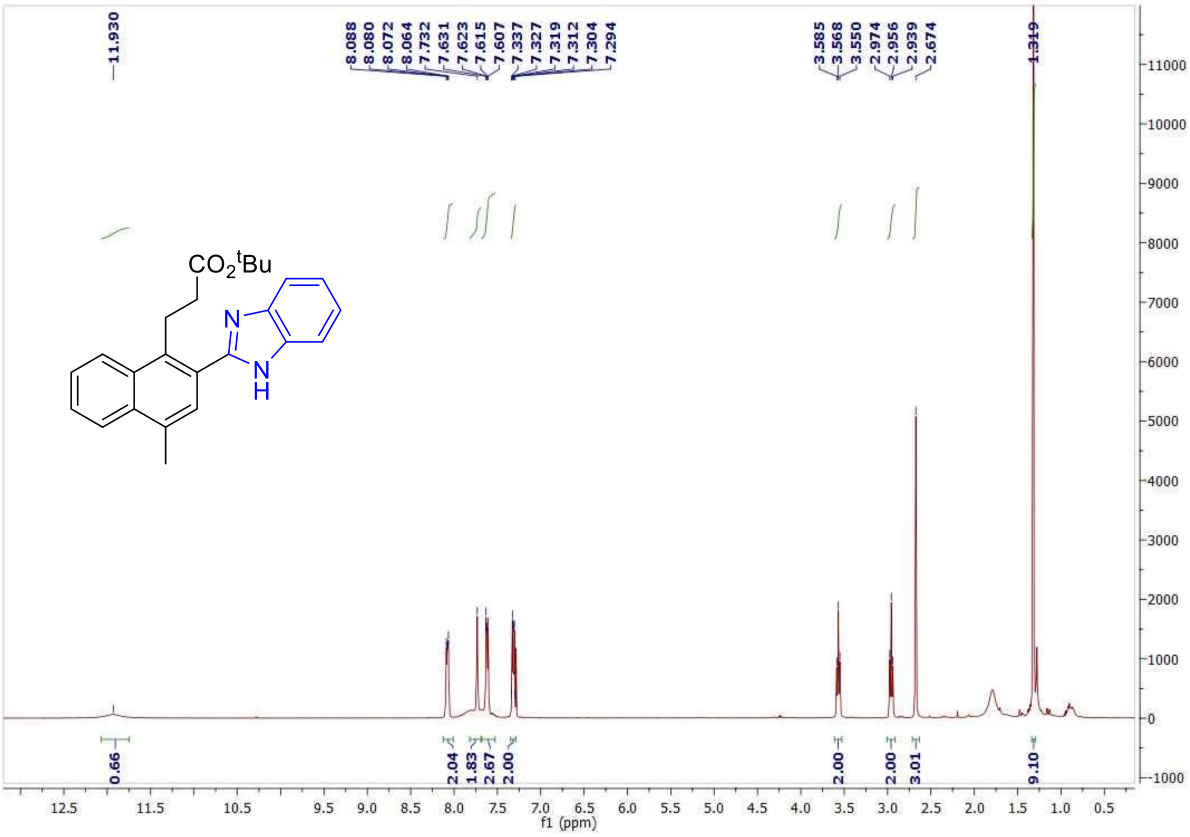

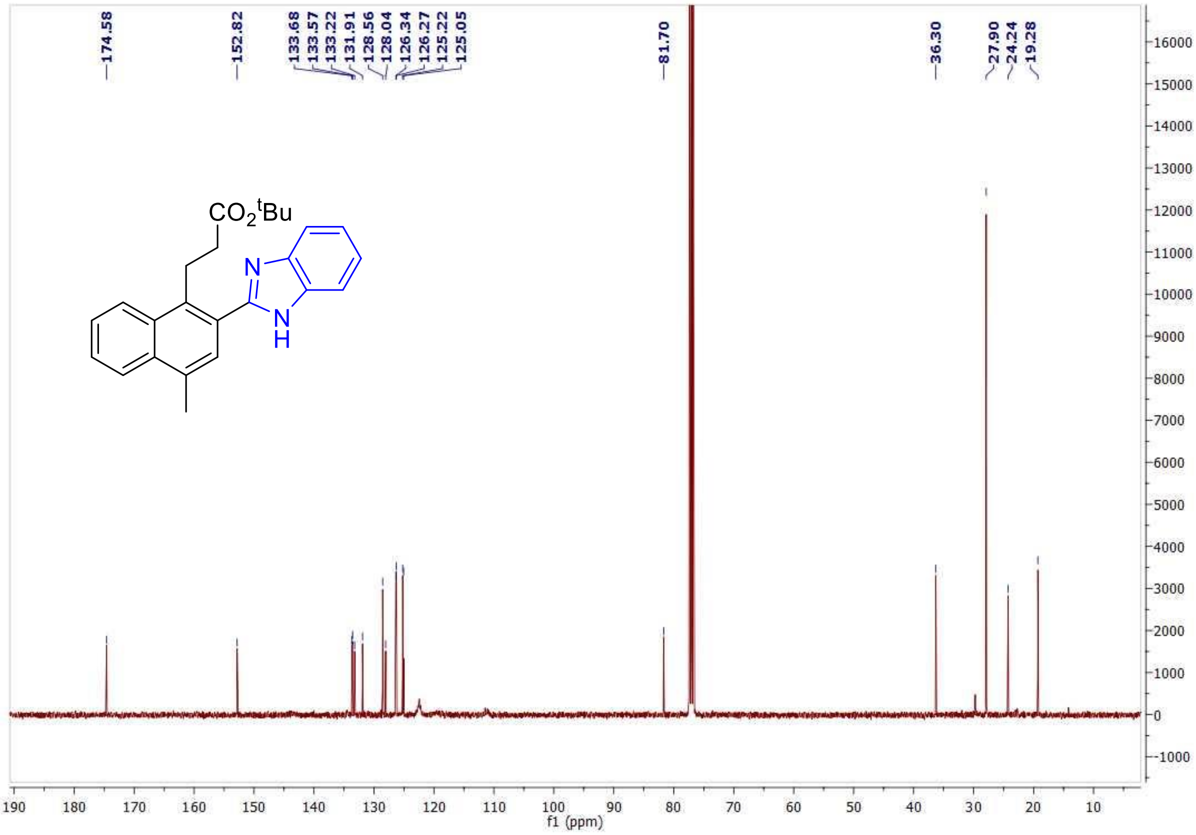

^{1}H and ^{13}C NMR of compound 5d

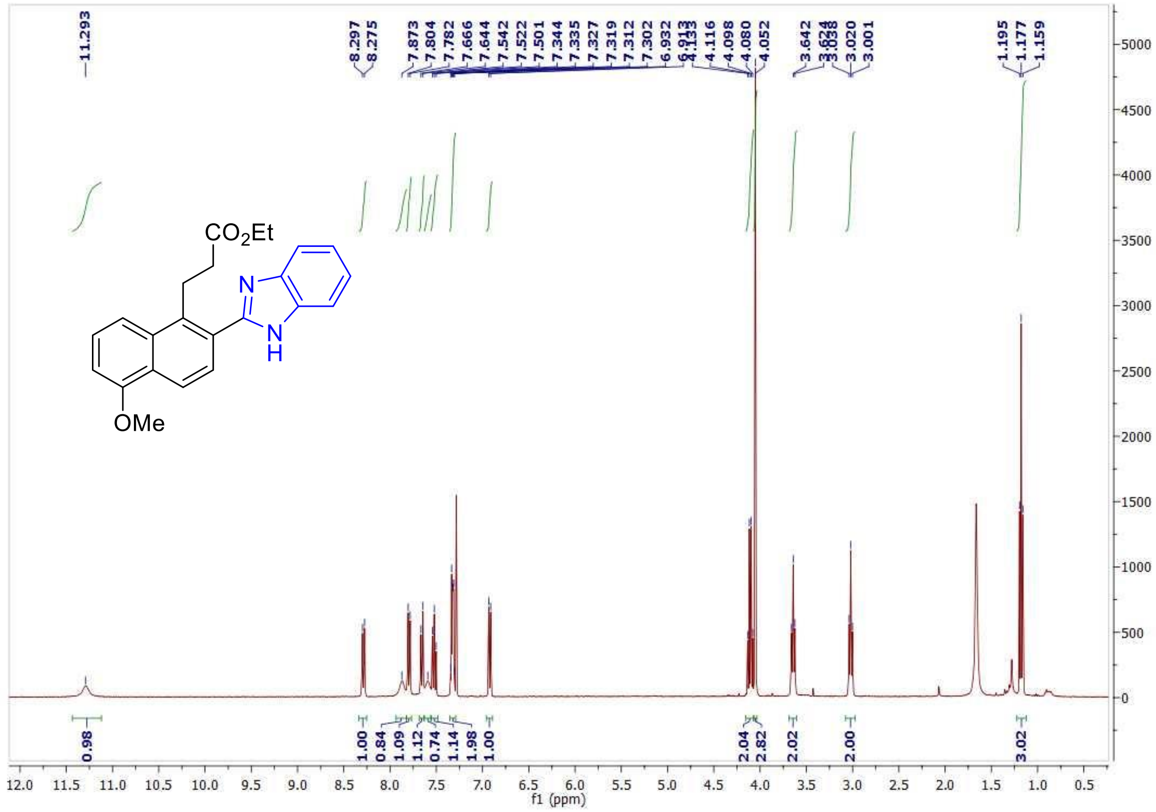

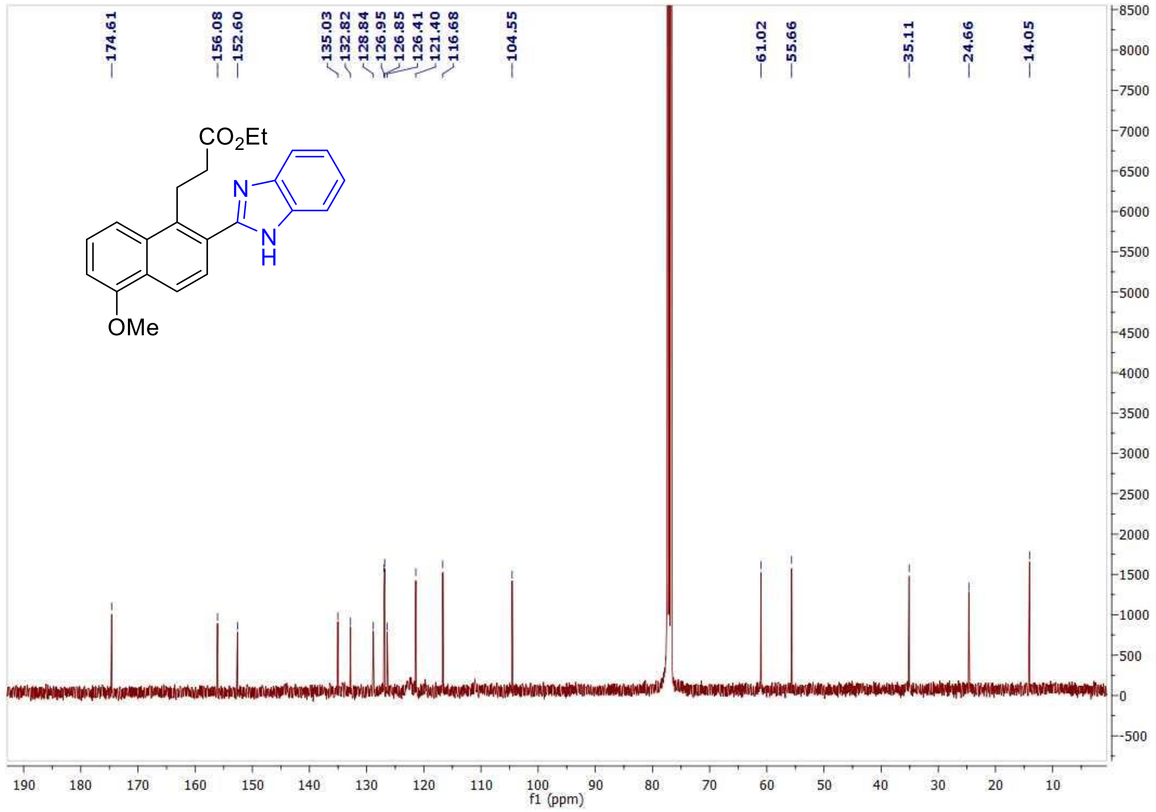

^{1}H and ^{13}C NMR of compound 5e

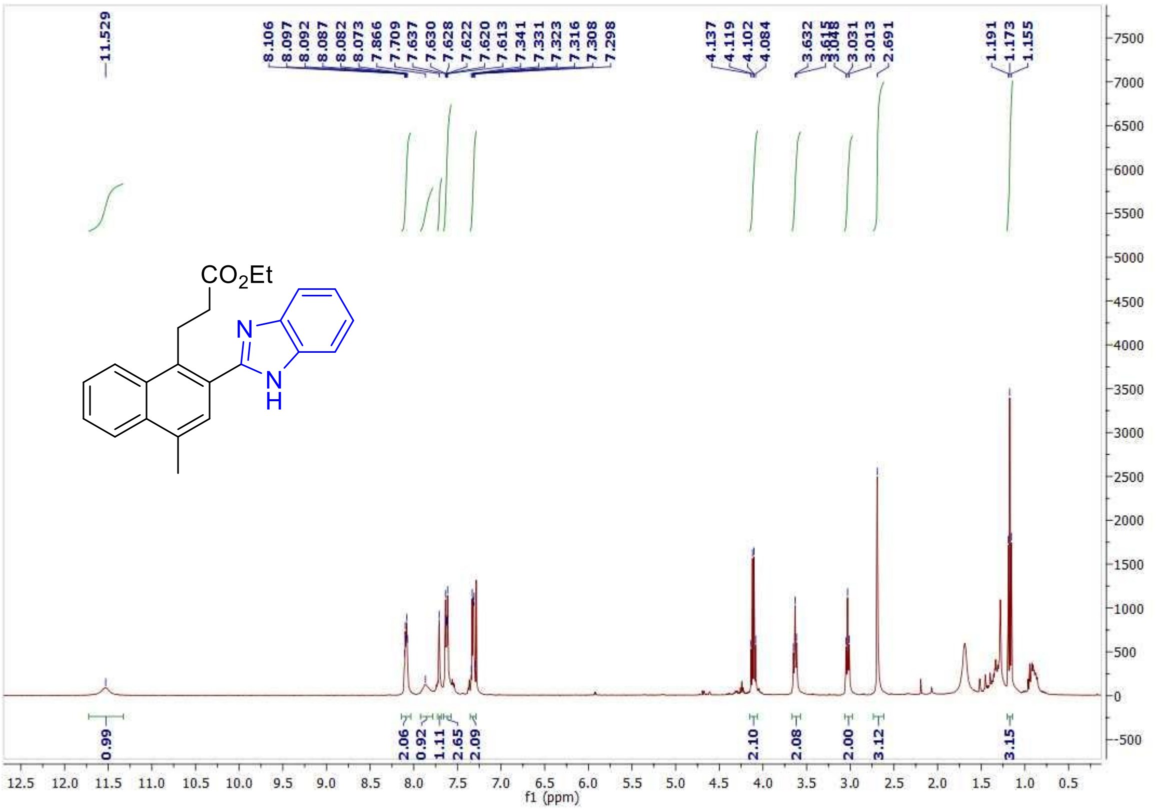
11.529
8.106
8.097
8.092
8.087
8.082
8.073
7.866
7.709
7.637
7.630
7.628
7.622
7.620
7.613
7.341
7.331
7.323
7.316
7.308
7.298
4.137
4.119
4.102
4.084
3.632
3.615
3.048
3.031
3.013
2.691
1.191
1.173
1.155
CO$_2$Et
N
N
H
0.99
2.06
0.92
1.11
2.65
2.09
2.10
2.08
2.00
3.12
3.15
12.5 12.0 11.5 11.0 10.5 10.0 9.5 9.0 8.5 8.0 7.5 7.0 6.5 6.0 5.5 5.0 4.5 4.0 3.5 3.0 2.5 2.0 1.5 1.0 0.5
f1 (ppm)
7500 7000 6500 6000 5500 5000 4500 4000 3500 3000 2500 2000 1500 1000 500 0 -500

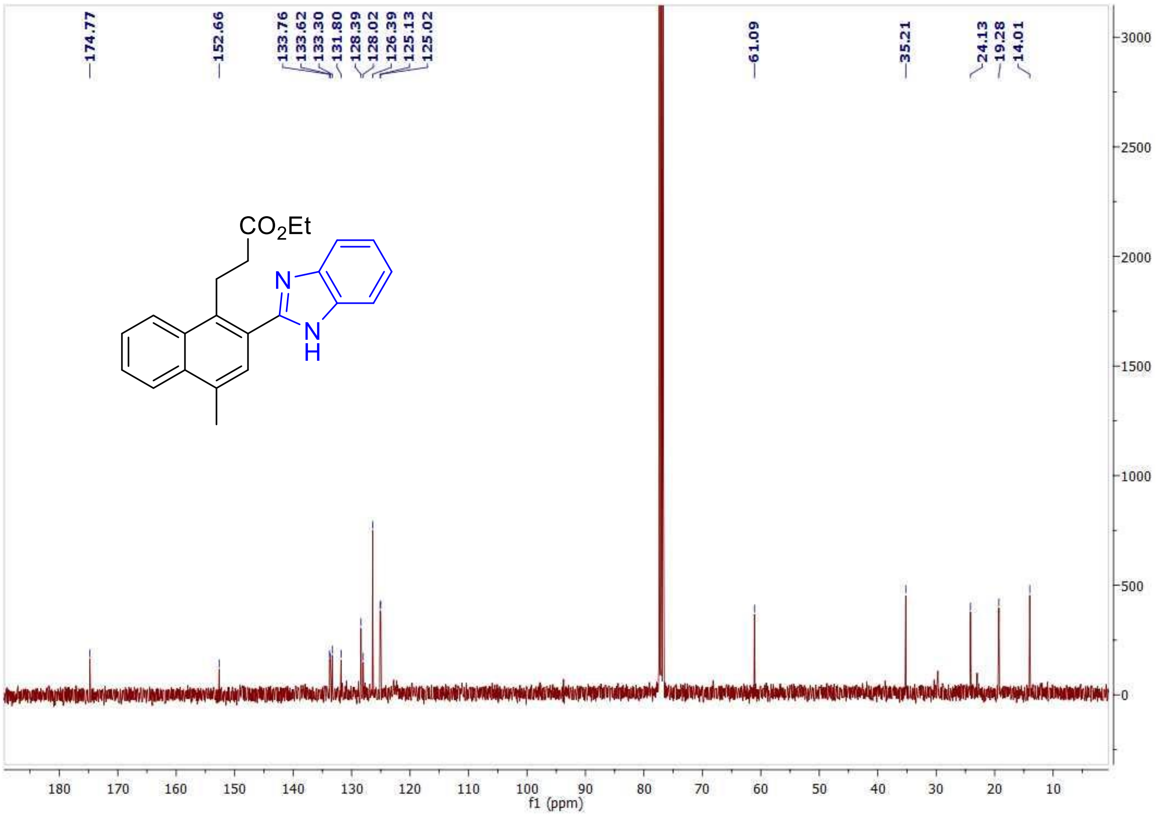
174.77
152.66
133.76
133.62
133.30
131.80
128.39
128.02
126.39
125.13
125.02
61.09
35.21
24.13
19.28
14.01
CO$_2$Et
N
N
H
180 170 160 150 140 130 120 110 100 90 80 70 60 50 40 30 20 10
f1 (ppm)
3000 2500 2000 1500 1000 500 0

6. Quantum chemistry geometry-optimised coordinates:

Coordinate of EBINP:

C	0.83167400	-2.55746100	0.17475900
C	2.19930600	-2.52217400	0.25329900
C	2.89445800	-1.31904500	-0.01539300
C	2.15809100	-0.14800400	-0.38548100
C	0.72363000	-0.20457300	-0.47554200
H	0.31588600	-3.49784800	0.34420400
C	4.32340300	-1.25708200	0.06977100
C	2.88600900	1.05213100	-0.64572900
C	-0.03380100	1.05481700	-0.84490400
C	4.25640800	1.07354900	-0.54682400
C	4.99354500	-0.07912700	-0.19095600
H	2.36290200	1.95959100	-0.91981400
H	4.79468800	1.99502200	-0.74842400
H	6.07311700	-0.02202300	-0.12795200
C	0.07169300	-1.40449500	-0.17791800
C	-1.39730700	-1.55999400	-0.18098000
N	-2.27655500	-0.98937800	-0.98005600
N	-2.00458200	-2.42874400	0.71626500
C	-3.51119000	-1.48329400	-0.59558000
C	-3.36495200	-2.39085000	0.48159200
H	-1.53953000	-2.89904900	1.47637700
C	-4.78638300	-1.21154600	-1.10843200
C	-4.45287100	-3.03357900	1.07495300
C	-5.87500700	-1.84904700	-0.52346400
H	-4.90608800	-0.52088500	-1.93664400
C	-5.71108100	-2.74492600	0.55254200
H	-4.33057400	-3.72635300	1.90205200
H	-6.87474300	-1.65537500	-0.90031100
H	-6.58579400	-3.22282600	0.98327800

H	0.50843000	1.59970400	-1.62033200
H	-1.00357000	0.79155200	-1.26399300
C	-0.23984000	1.99838200	0.36044400
H	-1.04310000	1.64710100	1.01254100
H	0.67194700	2.04021400	0.97059300
C	-0.51872600	3.42215700	-0.07831500
O	-1.41194300	4.02736300	0.73492700
O	0.01393700	3.96758500	-1.02439100
C	-1.71594000	5.41410400	0.44519900
H	-1.74100400	5.54961800	-0.63847300
H	-2.71828100	5.56228200	0.85371100
C	-0.70613100	6.34917600	1.09230100
H	0.28612000	6.20093300	0.65946500
H	-1.00149900	7.39007700	0.92360500
H	-0.65222100	6.17841100	2.17150400
H	2.76285400	-3.41100800	0.50921000
C	6.34391400	-2.45288400	0.51499300
H	6.61009200	-3.47232800	0.79731600
H	6.70907700	-1.75753600	1.28124600
H	6.81430100	-2.20785100	-0.44544000
O	4.92820000	-2.42894700	0.42206500

Coordinate of protonated EBINP:

C	0.45150900	-2.62233400	0.33833200
C	1.81002300	-2.76186600	0.35644300
C	2.64754900	-1.66461900	0.03449700
C	2.06457400	-0.40398200	-0.32281700
C	0.63633600	-0.26561800	-0.36247600
H	-0.14746100	-3.48280800	0.62159300
C	4.07100800	-1.80465300	0.06686600
C	2.93237600	0.68594400	-0.62544500
C	0.05191500	1.05743900	-0.79648700

C	4.29694400	0.51534700	-0.57529000
C	4.88033100	-0.72328800	-0.23550100
H	2.53241500	1.65798500	-0.88377200
H	4.94868200	1.35254700	-0.80368600
H	5.95907700	-0.81301200	-0.21406300
C	-0.16077100	-1.37497500	-0.00915800
C	-1.60213400	-1.28444600	0.01413900
N	-2.43989700	-0.32193100	0.01033800
N	-2.40180200	-2.66171000	0.03203200
C	-3.75609400	-0.80805800	-0.00702800
C	-3.79807600	-2.20594500	0.00177100
C	-4.94239400	-0.08181600	-0.02170000
C	-4.96516600	-2.94301700	0.00212200
C	-6.14077100	-0.80360900	-0.02845200
H	-4.92632600	1.00179800	-0.02793300
C	-6.15723800	-2.20334700	-0.01703700
H	-4.97715200	-4.02792100	0.01229000
H	-7.08234000	-0.26499600	-0.04213500
H	-7.10499300	-2.73011500	-0.02332600
H	0.68350600	1.49016000	-1.57319900
H	-0.93425700	0.91589100	-1.23789400
C	-0.06471200	2.08437400	0.35282600
H	-0.99724800	1.96574900	0.90777900
H	0.75338600	1.95079500	1.07171700
C	0.06066100	3.50867900	-0.16750800
O	-0.63565900	4.36760900	0.59098500
O	0.73664200	3.82037400	-1.12838800
C	-0.52929000	5.78148000	0.25228100
H	-0.49520300	5.87578300	-0.83499000
H	-1.45888100	6.21326000	0.62800300
C	0.68822400	6.41308200	0.90519200
H	1.60992600	5.98155900	0.50728400

H	0.69910100	7.48775900	0.69814100
H	0.66735200	6.27431700	1.98974700
H	2.26558000	-3.70555300	0.62883400
C	5.92694400	-3.26288200	0.46872000
H	6.04727500	-4.30621100	0.75875900
H	6.39854200	-2.61828000	1.21874400
H	6.39674200	-3.09837800	-0.50731700
O	4.51834500	-3.03727900	0.40752800
H	-2.13131800	-3.23402600	-0.77564900
H	-2.17962000	-3.19779000	0.87775200

Coordinate of deprotonated EBINP:

C	1.08531200	-2.46738800	0.22136900
C	2.44525000	-2.32672100	0.28645800
C	3.04631500	-1.07028600	0.01980200
C	2.20828400	0.03448700	-0.34673300
C	0.78450900	-0.14256300	-0.44418800
H	0.60640200	-3.41750800	0.42899800
C	4.45984800	-0.88109400	0.10796800
C	2.84226700	1.29136800	-0.59560300
C	-0.06596600	1.02609300	-0.90477600
C	4.20517200	1.43596500	-0.49431000
C	5.03803800	0.34783200	-0.14364200
H	2.24173900	2.15341200	-0.85812300
H	4.66079400	2.40458000	-0.68490400
H	6.10951400	0.49351400	-0.07528500
C	0.21888900	-1.38553900	-0.12202600
C	-1.22633400	-1.69379000	-0.10152000
N	-2.19980600	-0.74285500	-0.07809700
N	-1.63343300	-2.99014200	-0.05641900
C	-3.34491800	-1.48485100	-0.01914000
C	-2.99156900	-2.87798300	-0.00843500

C	-4.69455100	-1.09150100	0.03181600
C	-3.99506000	-3.86351700	0.04808200
C	-5.66968800	-2.08138900	0.08896200
H	-4.96146400	-0.03677000	0.02444700
C	-5.32298500	-3.45415300	0.09666800
H	-3.72935200	-4.91853000	0.05413000
H	-6.72068800	-1.80037300	0.12750000
H	-6.11508100	-4.19965700	0.14181100
H	0.48087400	1.63883400	-1.62593300
H	-0.95557500	0.64135000	-1.40455000
C	-0.55125300	1.90279500	0.25927300
H	-1.32125500	1.34632500	0.80460000
H	0.25664300	2.12332900	0.97015600
C	-1.12516800	3.22521000	-0.18396100
O	-1.71067000	3.87392700	0.86600800
O	-1.08366100	3.69939700	-1.30165300
C	-2.29604400	5.15573400	0.57760400
H	-2.75823100	5.12458400	-0.41254700
H	-3.07444600	5.28431500	1.33519500
C	-1.26350700	6.27279000	0.65459400
H	-0.50766300	6.14254600	-0.12358400
H	-1.74600000	7.24603400	0.50843800
H	-0.76808000	6.27692400	1.63047300
H	3.07641800	-3.16694200	0.55297700
C	6.57546500	-1.89104000	0.56547100
H	6.94195900	-2.88052200	0.84802300
H	6.87145800	-1.16507200	1.33584700
H	7.03674900	-1.59588200	-0.38751400
O	5.17359800	-2.00410900	0.45927600

7. References:

1 M. Sau, S. Dubey, J. Shaoo, G. Shaoo, P. Trivedi, A. Jana, S. Samanta and T. Das, *EurJOC.*, 2022, **2022(46)**, e202201188.

2 J. Hu and C. Zhang, *Anal. Chem.*, 2013, **85**, 2000-2004.

3 P. Kumar and H. B. Bohidar, *J. Fluoresc.*, 2012, **22**, 865-870.

4 L. G. Gagliardi, C. B. Castells, C. Rafols, M. Rosés and E. Bosch, *J. Chem. Eng. Data.*, 2007, **52**, 1103-1107.

5 Z. Wang, S. M. Richter, M. J. Rozema, A. Schellinger, K. Smith and J. G. Napolitano, *Org. Process Res. Dev.* 2017, **21**, 1501–1508.